0014-4754/95/080838-11$1.50 + 0.20

Shell microlaminations of the freshwater bivalve *Hyridella depressa* as an archival monitor of manganese water concentration: experimental investigation by depth profiling using secondary ion mass spectrometry (SIMS)

R. A. Jeffree, S. J. Markich, F. Lefebvre[a], M. Thellier[a] and C. Ripoll[a]

Environmental Science Program, Australian Nuclear Science and Technology Organisation, Private Mail Bag 1, Menai, New South Wales 2234 (Australia), Fax +61 2 717 9260, and [a]Laboratoire des Processus ioniques cellulaires, URA CNRS 203, Faculté des Sciences, Université de Rouen, F-76821 Mont-Saint-Aignan (France)
Received 3 August 1994; received after revision 4 November 1994; accepted 16 January 1995

Abstract. Specimens of the freshwater unionid bivalve *Hyridella depressa* were experimentally exposed to a synthetic river water containing an elevated Mn water concentration (20 mg l^{-1}) for 2 or 6 days. SIMS depth profiles through the incremental nacre microlaminations or tablets ($\sim$0.6 μm breadth) of the shells of these bivalves showed increases in the signal intensity of Ca-normalised Mn that corresponded to the period of exposure. These results support the proposition that bivalve shells can be used as retrospective monitors of water chemistry. They also indicate that 1) there is a lag phase between exposure to the elevated Mn water concentration and its expression in the shell, and 2) the period for Mn in the shell to reach equilibrium with the aquatic medium is greater that 2 to 6 days.
Key words. Bivalve; shell; microlamination; depth profiling; secondary ion mass spectrometry (SIMS); archival biomonitor; water chemistry; manganese.

Previous investigations[1,2] have indicated that the elemental composition of the annual incremental laminations that compose the shells of freshwater unionid bivalves, can reflect the elemental levels present in their aquatic medium at the time of shell construction. The shells of these long-lived organisms (up to 200 years for some species[1]) may therefore function as archival monitors of water chemistry and environmental change. In this study, this proposition is investigated over a daily, rather than an annual, time scale of shell construction. The depth profiling capability of the Cameca IMS 4f secondary ion mass spectrometry (SIMS) microprobe has been utilised to determine the effect of an elevated Mn water concentration on Mn levels in the microlaminations or crystalline tablets of the shell nacre of the Australian freshwater unionid bivalve *Hyridella depressa*.

Materials and methods

Collection, acclimation and preparation of specimens. Young adult specimens (shell length range: 37.4 to 45.7 mm) of the freshwater unionid bivalve *H. depressa*, approximately 1.5 to 3 years of age (determined by growth ring counts[3]), were randomly sampled from a minimally-polluted site in the Upper Nepean River, about 52 km south-west of Sydney (33°34'S, 151°15'E), New South Wales, Australia (see Jeffree et al.[4] for a location map). Specimens were transported to the laboratory within 1 h of collection and acclimated to a synthetic Nepean-Hawkesbury River water (pH 7.0 ± 0.1, 21.0 ± 0.1 °C, ~99% dissolved oxygen saturation) in a perspex aquarium (without substrate), under flow-through conditions for a period of 48 h without food (see Jeffree et al.[4] for a detailed description of the experimental system). An identification code was scribed onto the shell of each collected specimen.

Experimental design. After a 48 h acclimation period, several individuals were randomly selected (using random number tables) and used as controls, with the remaining bivalves then exposed to a constant Mn water concentration of 20 mg l^{-1}, which is a factor of ~260 times greater than the median contemporary Mn water concentration (0.075 mg l^{-1}) of the freshwater reaches of the Nepean-Hawkesbury River[4]. During experimental exposure to the elevated Mn water concentration, several specimens were randomly sampled (using random number tables) after 2 and 6 days, their soft tissues removed, and their shells thoroughly rinsed in high purity deionised water (Milli Q, 18 MΩ cm^{-1} specific resistivity) for at least 2 min, before being dried at room temperature.

Manganese was selected in the present study because 1) it is known to have a high concentration ratio, relative to many other elements, in the shell of freshwater bivalves[5,6], and 2) preliminary laboratory measurements revealed no significant ($p \leq 0.05$) change in the valve movement behaviour of *H. depressa*, measured in terms of the mean duration and amplitude of shell valve gape (see Brown et al.[7] for more detail), when exposed to the

elevated Mn water concentration for periods of up to 6 days, relative to the background Mn water concentration. These measurements of shell movement also indicated that exposure of specimens without food did not appear to cause any adverse behavioural/physiological effects.

Chemical analysis and geochemical modelling of the experimental waters. Throughout the experimental exposure period, triplicate water samples were collected daily, and the concentration of Mn then analysed using a Labtam 8410 inductively coupled plasma atomic emission spectrometer (ICP-AES), as described by Jeffree et al.[4]. Other metals and anions were also measured using various analytical techniques (see Markich and Jeffree[8] for more detail) to confirm the nominal synthetic water composition; the mean values of all parameters were within 10%, but usually within 5%, of their nominal values. Manganese was added to the synthetic water as the chloride salt ($MnCl_2 \cdot 4H_2O$), resulting in an increase in chloride concentration by a factor of ~ 1.5 relative to the background; however this factor of increase in chloride water concentration is within its natural range of variation for the freshwater reaches of the Nepean-Hawkesbury River[9,10].

Geochemical modelling of Mn in the synthetic river water, using the speciation code HARPHRQ[8,11], predicted that the free (hydrated) ion (i.e. Mn^{2+}) was predominant in both the background ($\sim 99\%$) and elevated ($\sim 97\%$) Mn exposures. The free metal ion is generally considered the most biologically available metal species[12,13]. Therefore, based on the predicted speciation of Mn, it may be expected that this metal would be present in the synthetic river water in its most bioavailable form for uptake into the soft tissue and shell of *H. depressa*, thus maximising Mn uptake under these experimental conditions.

Preparation of shell sections for SIMS depth profiling analysis. For each selected specimen (i.e. control or Mn exposed) a small piece of shell, with a surface area of about 5 mm × 10 mm, was cut from the posterior-ventral region of the right valve, a section of the shell that provided an axis of maximal growth and a near flat area. The whole shell section was then transversely cut into several sections of about 1 mm in breadth. Each of these sections were then mounted on a round (1 cm diameter) glass slide with a heat-sensitive adhesive (Crystal bond, Leco), whereby the outer surface (periostracum) was facing upward. Prior to mounting, the glass slide and each shell section were precisely measured with a digital vernier (Mitutoyo; to three decimal places), and again as a total breadth after mounting, to establish the breadth of the mounting medium. This was necessary to accurately determine the final breadth of the shell section after grinding. Each shell section was then slowly ground from the outer surface (periostracum) using a hand lapping tool and then polished (using a Buehler Minimet polisher with a 69-1560 Minimet precision attachment) until a breadth of 20 to 30 μm (measured with the digital vernier) was achieved. Each shell section was then removed from its mounting medium and cleaned with acetone prior to depth profiling analysis using SIMS.

SIMS depth profiling analysis of shell sections. SIMS is based on the fact that charged atomic and molecular species (i.e. secondary ions) are ejected from the surface of a condensed phase (liquid or solid) under particle bombardment and sorted by mass spectrometry (see reviews by Thellier et al.[14] and Stingeder[15]). SIMS depth profiles[14] were performed using a CAMECA IMS 4f ion analyser. Sputtering[14], a process of removing individual atoms from a sample surface, was carried out by bombarding the specimen surface with fast O_2 molecules (fast atom bombardment (FAB) source of the IMS 4f instrument) produced by electrical neutralisation of a primary O^{2+} ion beam. Before neutralisation, the primary current was 6 μA, and the ion energy was 15 keV. The diameter of the surface area subjected to O_2 bombardment was ~ 1000 μm, and that of the analysed area 250 μm. The measurements were carried out using the following settings: field aperture 1800 μm (FA1), contrast aperture 400 μm (CA1), transfer lens 250 μm. The advantage of using the FAB/SIMS combination is that the primary neutral beam of the FAB source minimises electrical charging from the shell (an insulator), and hence permits stable count rates.

The sputtering rate of the ion beam was calculated from a knowledge of 1) the total depth of the sputtered hole in the shell of two sample specimens, and 2) the time period of sputtering (i.e. 2.5 h). The depth of the sputtered hole was calculated from a knowledge of the angle of inclination of the shell sections on the sample stage of the scanning electron microscope (SEM) (see below), coupled with the internal measurement scale of the SEM. This procedure was performed at several different angles of inclination and magnification scales to derive a mean sputtering rate for each specimen. Based on two different depth measurements, the sputtering rates (mean $\pm$ SE; $n = 6$) were 1.55 ± 0.12 and 1.63 ± 0.10 μm in 2.5 h, corresponding to a mean sputtering rate of ~ 11 nm min^{-1}. Indeed, by using the measured value of the mean sputtering rate, it is a simple procedure to convert irradiation times into profile depths.

Preparation of transverse shell sections for examination of their microstructure. To examine the microstructure of the shell, several control and Mn exposed specimens were prepared as follows. The left shell valve of the specimen was dipped into a standard mix of 5:1 Araldite D: Hardener HY956 (Ciba Geigy), then removed and allowed to dry. This procedure provided a hard coating to prevent the shell valve from shattering when cut with a fine jewellers saw. The shell valve was

dry cut along the axis of maximum growth (i.e. from the umbo to the posterior-ventral margin), with another cut made to provide a slice about 5 mm in breadth. The transverse shell slice was then mounted in the Araldite D/Hardener mix and ground using SiC papers and distilled water, before being polished (~0.25 μm) with diamond paste and a lubricant of 1,2-ethanediol (ethylene glycol). Samples progressed through several cycles of both grinding and polishing and were sonic cleaned with alcohol between each cycle. Two shell sections were not polished so that their fractured surface could be observed. Polished and fractured transverse sections of shell were then carbon-coated and examined with a JEOL JXA-840 scanning microanalyser (operated at an acceleration voltage of 15 keV and at various magnifications) to determine their microstructure, including the breadth of the shell nacre microlaminations, particularly those at the growing edge where SIMS depth profiles were performed.

Results

Shell microstructure and composition. The precise evaluation of the capability of the shell of *H. depressa*, and indeed the shells of other bivalve species, to act as an archive of the living animals' aquatic environment, requires a thorough knowledge of the shell's microstructure and composition. Figure 1 shows scanning electron micrographs of transverse shell sections of specimens of *H. depressa* used in this investigation. The shell of *H. depressa* is comprised of three distinct layers i.e. a thin outer organic layer or periostracum (P), a middle (prismatic, Pr) and an inner (nacreous, N) layer (see fig. 1a), where both the latter layers are composed of $CaCO_3$, in intimate association with an organic matrix (confirmed by using an energy dispersive X-ray analyser (EDX: Tracor Northern TN 5402) attached to the SEM).

Molluscan shells contain two common mineral polymorphs of $CaCO_3$, calcite and aragonite. As an initial visual determination of the exact nature of the $CaCO_3$

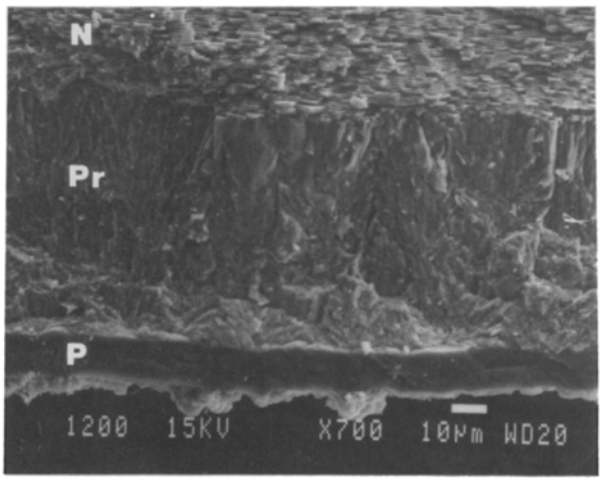

a

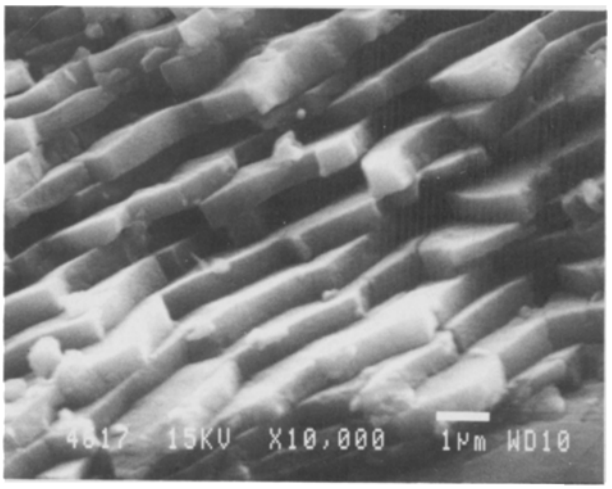

b

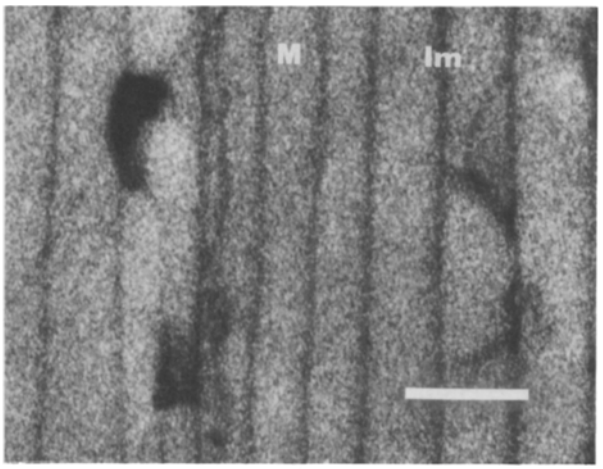

c

Figure 1. Scanning electron micrographs of transverse shell sections of typical specimens of *H. depressa*, showing
a a fractured section of shell with three distinct layers i.e. a thin outer organic layer or periostracum (P), a middle (prismatic, Pr) and an inner (nacreous, N) layer (×700);
b a higher magnification (×10,000) of the nacreous layer shown in *a*, displaying 1) a 'brick-wall' depositional pattern of thin regular microlaminations or tablets (the organic matrix between the individual layers is not evident), and 2) a subconchoidal fracture, characteristic of aragonite; and
c a polished section of shell from the nacreous layer (×20,000) of a specimen exposed to the elevated Mn water concentration for 6 days, displaying microlaminations (M) of ~0.6 μm in breadth (horizontal scale bar represents 1 μm; the right side is the growing edge) surrounded by an organic (i.e. interlamellar, Im) matrix.

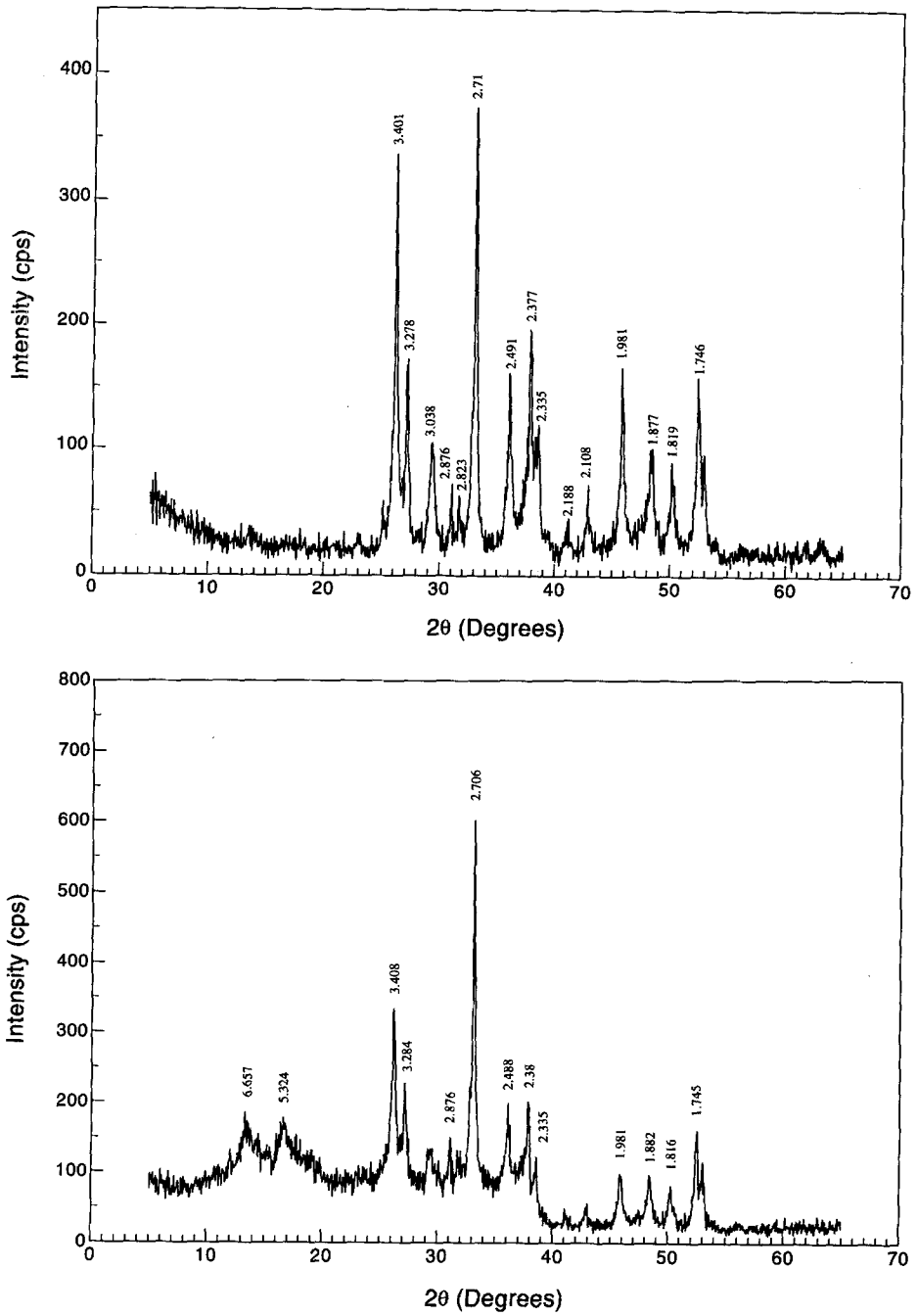

Figure 2. Typical X-ray diffractograms for the *a* nacreous and *b* prismatic layers of the shell of *H. depressa*, confirming that both layers are composed of aragonite, with no detectable calcite. A small amount of contamination is evident in *b*, and was most probably introduced as a result of the sampling method used in obtaining shell powder from this layer (located between the periostracum and the nacreous layer; see fig. 1a).

in the shell of *H. depressa*, Meigen's stain was applied to several thin polished shell sections according to the method described by Suzuki et al.[16] and examined by SEM. For all shell sections, both the prismatic and nacreous layers stained positive, indicating that the mineralogy of both layers was aragonite. Moreover, the specific mineralogy of both of these layers was reconfirmed by X-ray diffractometry (XRD) (see fig. 2a and 2b), whereby dried homogeneous shell powder (~ 0.1 to 0.3 g) from each layer was mixed into a slurry with amyl acetate and an adhesive, smeared-mounted on a glass slide and then analysed with a Siemens D500 X-ray diffractometer (utilising a Cu Kα radiation, set to run from 5° to 65° 2θ at 0.05° increments and operating at 40 kV and 30 mA). The resulting X-ray diffractograms were compared to a standard orthorhombic

aragonite (41-1475) and rhombohedral synthetic calcite (5-586) as a guide[17].

The prismatic layer can best be described as having an irregular simple microstructure (terminology after Carter[18]), whereby columnar aragonite prisms are oriented almost perpendicular to the inner surface of the shell (fig. 1a). These prisms are also notable for their diverging longitudinal striations, giving the prism a feathery appearance. In contrast, the nacreous layer consists of thin horizontal lamellae (microlaminations), each composed of tabular crystals of aragonite deposited on a sheet of organic matrix (conchiolin) lying almost parallel to the inner shell surface (fig. 1a, 1b and 1c). The breadth of each lamellae is ~0.6 μm in diameter (fig. 1b and 1c). The organic matrix (conchiolin) occurs as thin (0.05 to 0.08 μm) adventitious sublayers within the nacreous layers (interlamellar matrix). The prismatic and nacreous aragonite layers invariably maintain a sharp mutual boundary without microstructural intergradation (fig. 1a).

Figure 1b shows a higher magnification of the nacreous layer shown in figure 1a, displaying 1) a 'brick-wall' depositional pattern, where crystals in each layer usually develop in offset positions from those of the layer immediately below, and 2) a subconchoidal fracture, characteristic of aragonite. Figure 1c shows a polished section of shell from the nacreous layer of a specimen exposed to the elevated Mn water concentration for 6 days. It is evident from this shell section that the microlaminations or nacre tablets near the growing edge (right side) are relatively uniform in breadth (~0.6 μm), indicating no apparent change in the rate of shell deposition, relative to previously deposited microlaminations. This phenomenon was also observed in other sections of the shells of bivalves exposed to the elevated Mn water concentration for either 2 or 6 days.

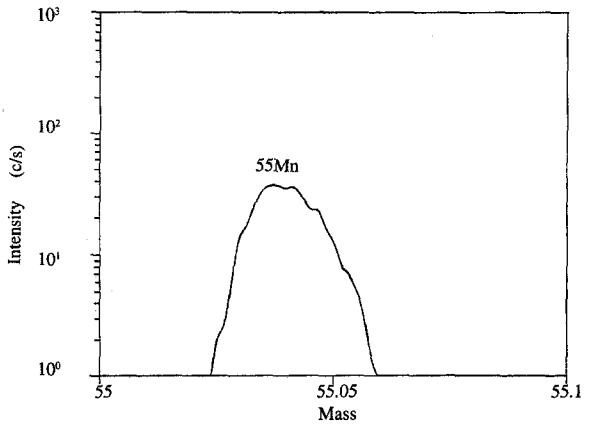

Figure 3. High resolution ^{55}Mn peak for the shell nacre of a typical specimen of *H. depressa* exposed to the elevated Mn water concentration for 6 days, showing no spectral interferences.

SIMS spectral analysis of shell sections. Initial SIMS spectral analysis (for elements ranging in atomic mass from 1 to 150) was performed on the internal surface of a shell from a bivalve exposed for 6 days to the elevated Mn water concentration. Figure 3 shows the interference-free, high resolution peak of ^{55}Mn from initial spectral analysis. Experimental results confirm that Mn was accumulated in the shell during the Mn exposure period, and was easily detected by this technique. Like ^{55}Mn, the spectra for ^{40}Ca also appeared to be free of interferences; however a small ^{56}Fe peak showed an interference from ^{40}CaO (the ^{40}Ca and $^{40}CaO/^{56}Fe$ spectra are not shown here; see Thellier et al.[14] and references therein). A typical signal intensity for the ^{55}Mn peak of ~10^4 counts per second (c/s) was observed, with a higher signal intensity (10^5 to 10^6 c/s) for the ^{40}Ca peak. Therefore, ^{55}Mn and ^{40}Ca (hereafter referred to as Mn and Ca) were investigated in subsequent depth profiles through the shells.

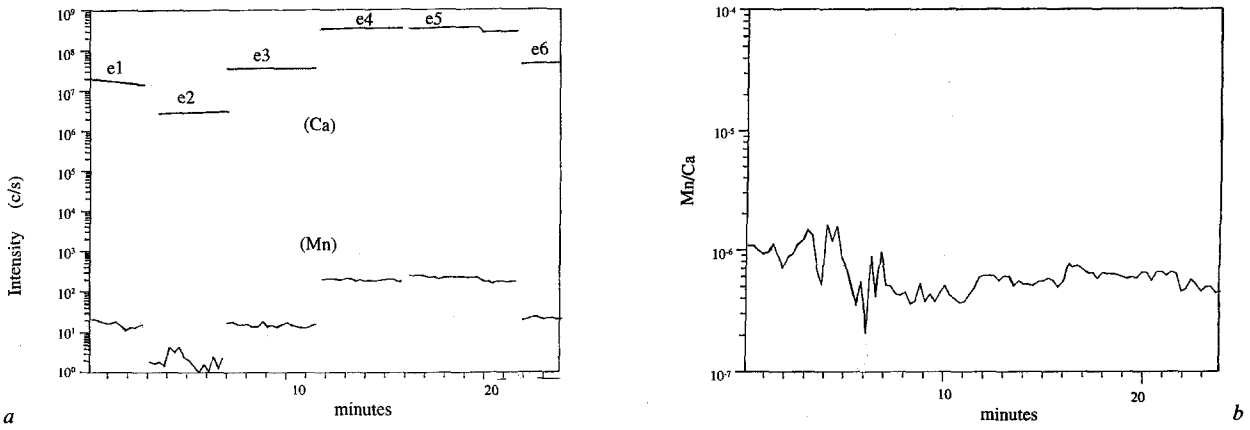

Figure 4. Shell nacre surface signal intensity of *a* Ca and Mn, and *b* the ratio of Mn to Ca signal intensity, showing the variability in lateral distribution of these measured signal intensities in a typical control shell:e1 to e6 represent different areas on the inner nacre surface of the shell. Due to a very low Mn signal intensity in area e2, the Mn signal pattern is comparatively noisy.

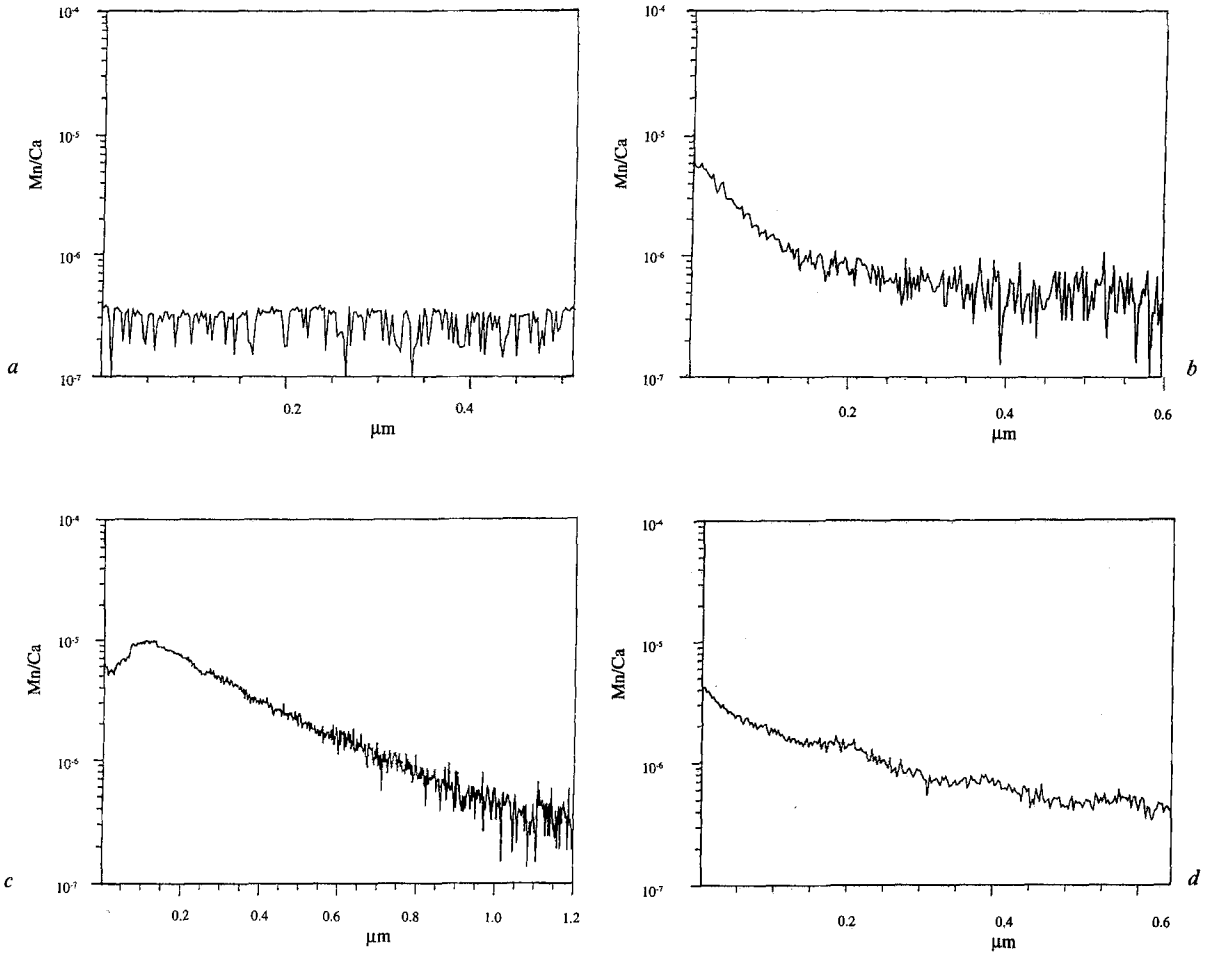

Figure 5. Normalised depth profiles of Mn through the shell nacre of *a* a typical control specimen, and typical specimens of *H. depressa* exposed for *b* 2 days, and *c* and *d* 6 days, to the elevated Mn water concentration.

SIMS depth profiling analysis of shell sections. Figure 4a shows the signal intensities of Ca and Mn in several areas of the inner (nacre) surface of a typical control shell; a high and coincident variability of the signal intensities of both metals was observed. This result may be due to SIMS effects (e.g. electrical charging, matrix effects) or to natural surface heterogeneity, in combination with the fact that Mn is treated as a metabolic analogue of Ca in this and other species of freshwater bivalves[8]. Both of these interpretations are consistent with the finding that the ratio of the Mn to Ca signal intensity was relatively constant over the entire surface (fig. 4b). As a consequence, in the results reported below, the Mn signal intensity will be shown as the normalised Mn/Ca signal intensity. The advantage of expressing the results as a (Mn/Ca) ratio is that any 1) biological variables which influence the metabolic pathway, or 2) physical/analytical variables (e.g. SIMS effects), will not disturb the ratio as much as they would influence absolute values.

Figure 5 shows typical normalised (Mn/Ca) depth profiles in a control shell (fig. 5a) and in shells from specimens that were exposed for 2 days (fig. 5b) or 6 days (fig. 5c and 5d) to the elevated Mn water concentration. Figure 5a shows that the normalised Mn signal intensity ($\sim 3 \times 10^{-7}$) is constant throughout the entire depth profile. Based on four replicate depth profiles of a typical control shell (not shown), it was concluded that the normalised Mn signal pattern was constant throughout all the depth profiles, however, each depth profile showed a variable normalised (basal) Mn signal intensity i.e. 0.1×10^{-7}, 3×10^{-7}, 0.2×10^{-7} and 6×10^{-7}. From these data, the basal normalised Mn signal intensity was estimated to be in the range $2.5 \pm 2.4 \times 10^{-7}$. Moreover, from the normalised Mn depth profiles in the shells of specimens exposed to the elevated Mn water concentration, for either 2 or 6 days (fig. 5b, 5c and 5d), one may observe that 1) at the beginning of the depth profiles (left side), the normalised Mn signal intensity exceeded that of the control, 2) the normalised Mn signal intensities were of approximately equal value both in the 2 and 6 day exposed specimens, and 3) the normalised Mn signal intensities tended to decrease with in-

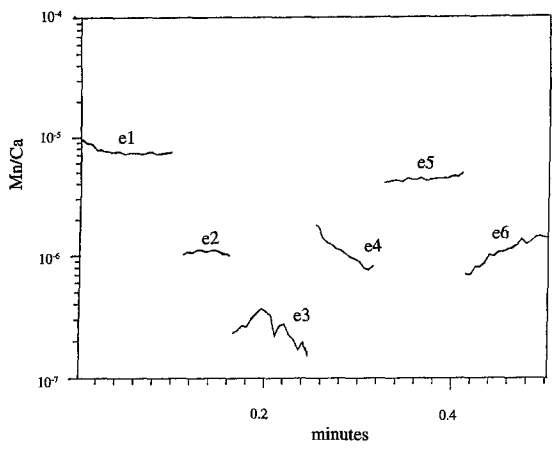

Figure 6. Normalised Mn signal intensity in different areas (e1 to e6) of the inner nacre surface of a shell from a typical specimen of *H. depressa* exposed for 6 days to the elevated Mn water concentration.

creasing depth (i.e. from left to right) from the shell surface.

Figure 6 shows the beginning of normalised Mn depth profiles in different areas on the inner (nacre) surface of shells from specimens exposed for 6 days to the elevated Mn water concentration. In contrast to what was observed from the shell of a typical control specimen (fig. 4b), the normalised Mn signal intensity was relatively variable from one area of the shell to another (i.e. 2×10^{-7} to 2×10^{-5}) compared to the basal level (i.e. $2.5 \pm 2.4 \times 10^{-7}$).

Discussion

The results of the present investigation conclusively demonstrate that there is a positive response in the Ca-normalised Mn signal intensity in the shell nacre of *H. depressa* exposed to the elevated Mn water concentration (i.e. 20 mg l^{-1}). This result is consistent with the assertion of previous investigations[1,2], that the shell nacre of freshwater bivalves can operate as an archival monitor of element concentrations in the aquatic environment. Details of the underlying rationale for the advantageous use of shell nacre in bivalves, as an important means of indicating the bioavailable fraction of a metal in the organism's aquatic environment, is discussed elsewhere[19].

Furthermore, our results confirm that the microstructure (fig. 1a, 1b and 1c) and mineralogy (fig. 2a and 2b) of the shell of *H. depressa* is consistent with that of other freshwater unionid bivalves (see reviews by Carter[18] and Watabe[20]), where the nacreous and prismatic layers are composed of aragonite, with the former layer consisting of incremental lamellae (i.e. microlaminations). Fritz and Lutz[21] clearly demonstrated that these incremental lamellae were deposited at a rate of *approximately* one per day in the freshwater bivalve *Corbicula fluminea*, a finding that receives general support in the literature[21,22]. However, there is also evidence that some species of marine bivalves (e.g. *Pinctada margaritifera*) can deposit multiple (up to 25) incremental lamellae on a daily basis (see Caseiro[23] and references therein). Indeed, the factors influencing the rate of deposition of the incremental lamellae, such as bivalve age, season, locality etc, are reviewed elsewhere[22], and should be carefully considered when interpreting incremental lamellae as archives of water chemistry. The presence of these incremental lamellae in the shell of *H. depressa*, which can respond to an elevated Mn water concentration within a period of days, indicates the possibility that pollution events that are archived in the microlaminations of the shell could be potentially dated to within very small periods of time.

However, our results also indicate that the following two factors should also be considered, with respect to the use of bivalve shells in this role:

1) Lag in response time. The results of SIMS depth profile analysis through the shells of specimens exposed for 2 or 6 days to the elevated Mn water concentration, indicate that Mn falls to background levels within a distance of about 0.4 to 1.1 µm, or about 1 to 2 microlaminations (fig. 5b, 5c and 5d). Assuming that each microlamination represents approximately one day of shell growth (see above), then there is a delay in response to the elevated Mn water concentration of up to several days, before there is a discernible increase in Mn signal intensity.

2) A shell/water equilibration period. Isotopic equilibrium between bivalve shells and their aquatic environments is well established[24–26]. However, based on the patterns of increase in the normalised Mn signal intensities of shell depth profiles in specimens exposed to the elevated Mn water concentration, it is not obvious that an equilibrium level of Mn has been reached in the shells of these specimens within the 6 day exposure period (fig. 5b, 5c and 5d), a finding generally consistent with that of Dillaman and Ford[27] working with *Mercenaria mercenaria* exposed to ^{45}Ca. This is particularly obvious from figure 5b and 5d, an obvious contrast to the relatively stable normalised Mn signal intensity shown for the typical control shell (fig. 5a). However, these results also show that the normalised Mn signal intensities in the shells of bivalves exposed for either 2 or 6 days were of approximately equal magnitude. This suggests that the rate of incorporation of Mn during the exposure period is not closely synchronised between individuals, at least over these short periods of exposure to the elevated Mn water concentration. This conclusion is consistent with the variable individual rates of uptake of metals into the tissue of this and other freshwater bivalve species during similar short-term experimental exposures[8,28].

The greater spatial heterogeneity in the normalised Mn signal of the inner nacre surface of the shell of one of the 6-day exposed specimens (fig. 6), relative to the control shell (fig. 4b), would also suggest that even within an individual, different regions of the shell-secreting mantle have different short-term metabolic rates of response to the elevated Mn water concentration. Indeed, regional variations in the metabolic activity of the mantle, and hence its ion flux rates, have been confirmed in the literature for several bivalve species[25,29,30]. For example, there is a greater metabolic activity in the marginal region, than in the central region of the mantle. Since the shell pieces cut from the valves of specimens covered a relatively large proportion of the valve, due to the animals' small size, the above interpretation may hold true. However, there was no apparent difference in the rate of shell deposition, based on the breadth of the most recently formed microlaminations, between different regions of the shell pieces (a typical section is shown in figure 1c). Therefore, it follows that the normalised Mn signal intensity per unit area of shell is a function of two variables (i.e. shell deposition rate and Mn flux rate) that can be considered independent, within limits: a unit change in Mn/Ca secretion (i.e. flux rate) need not result in a uniformly proportional change in the rate of shell deposition.

An alternative interpretation of the greater spatial heterogeneity in the normalised Mn signal intensity on the inner nacre surface of the specimen (fig. 5) exposed to the elevated Mn concentration, may be related to processes of crystal growth, whereby new crystal growth occurs by the addition of ions to the existing crystal faces, in a process that is not necessarily spatially uniform[31,32]. Indeed, the greater spatial heterogeneity observed may be due to the ion probe sputtering newly formed mineral deposits scattered over the matrix of the growing surface, which may be closer to reaching equilibrium than the older underlying surface deposits (see fig. 3.4 in Lowenstam and Weiner[25] for a conceptual overview). The phenomenon of spatial heterogeneity is not only confined to the shell surface. This natural phenomenon has also been well described for a variety of elements throughout the entire depth of bivalve shells[29,33]. For this reason it is paramount to establish the baseline variation of the level of an element in the shell (see 'Results'), before being able to discern whether the element is at an elevated level.

Longer-term experimental exposures will be required to determine 1) the period of time before equilibrium is reached, and 2) the specific rates of deposition of the incremental microlaminations. However, previous experimental studies of Ca uptake into the tissues of this and related species of Australian freshwater bivalves indicate that the period required to attain equilibrium between the aquatic medium and the body fluids is greater than 20 days[8,28]. Further details concerning molluscan shell structures and biochemical and physiological aspects of their formation are reviewed elsewhere[20,34,35].

Our interpretation of an increase in the normalised Mn signal intensities for the shells of specimens exposed to the elevated Mn (i.e. Mn/Ca) water concentration for either 2 or 6 days, is most likely due to Mn being treated as a metabolic analogue of Ca during its direct uptake from the aquatic medium[8], and subsequent transfer across the mantle for shell construction. Previous studies employing electron paramagnetic resonance (EPR) spectroscopy have shown that Mn^{2+} is incorporated into the lattice of calcite and aragonite in the bivalve shell by substitution at Ca^{2+} sites[36–38], most probably in the form of a solid solution[39–41]. This mode of incorporation into biogenic aragonite and calcite has also been demonstrated for several other metals, such as Sr and Mg[29,42,43]. The calcite lattice, however, can more readily accommodate Mn^{2+} (and other metal ions with an ionic radius smaller than Ca) at Ca^{2+} sites, compared to the aragonite lattice; the converse is true for metal ions which have an ionic radius larger than that of Ca (e.g. Sr). This phenomenon arises because Ca^{2+} has a six-coordinate structure with its nearest oxygen atoms in calcite, whereas in aragonite it has a nine-coordinate structure (i.e. a more open crystal lattice and greater Ca–O bond distances)[37,44]. For example, Mn^{2+} is more readily accommodated into calcite (as opposed to aragonite) because it forms a six-coordinate carbonate (i.e. rhodochrosite; $MnCO_3$), that is isostructural with calcite. Thus, crystal structure is a priori a significant controlling factor in metal uptake potential[33,45]. Studies employing techniques such as X-ray and electron diffraction and X-ray absorption spectroscopy, will further improve our knowledge of the mode and nature of metal ion incorporation into biogenic aragonite and calcite.

Manganese, like other trace metals, is bound both within the organic matrix and the aragonite/calcite lattice of bivalve shells[29,46]. By employing a convenient method for estimating the organic-bound and crystal-bound proportion of a metal in bivalve nacre, Lingard et al.[46] demonstrated that Cd and Pb were predominantly associated with the aragonite lattice of the freshwater unionid bivalve *Elliptio complanata*, with only a minor proportion of each metal bound to the organic matrix. Indeed, the organic matrix would be expected to contain some proportion of a metal, such as Ca or Mn, since it forms the platform for crystal formation[47–49].

Since the microstructure and mineralogy of *H. depressa* and *E. complanata*[50] are very similar, we predict a priori that the partitioning of Mn in the nacre of *H. depressa* will follow a similar pattern to that described for Cd and Pb in *E. complanata*[46]. The rationale for this prediction is described as follows. In comparison to either Cd

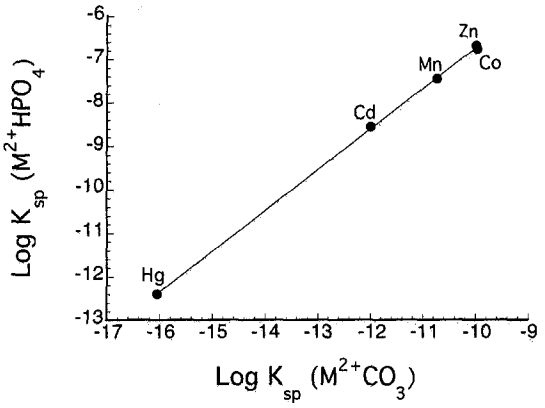

Figure 7. Simple linear regression analysis showing the logarithms of the solubility products (log K_{sp}) of Hg, Cd, Mn, Co and Zn carbonate versus their corresponding log K_{sp} for hydrogen phosphate. The simple linear regression equation is $M^{2+}HPO_4 = 0.936(M^{2+}CO_3) + 2.638$; $r^2 = 0.999$, $p \leq 0.001$, $n = 5$.

or Pb, Mn generally has a lower binding strength (i.e. smaller formation constants; see Smith et al.[51]) with O, P, N and S functional groups, which are characteristic of the major ligands (i.e. proteins, polysaccharides, sulphated mucopolysaccharides etc.) comprising the organic matrix of the nacre[35,49]. In contrast, however, Mn has a relatively smaller partition coefficient (i.e. ratio of the concentration of an element in shell to that in the extrapallial fluid) in biogenic aragonite than either Cd or Pb (i.e. Cd > Pb > Mn[6]; see also Onuma et al.[52]). This is due to Mn being structurally less favoured than Cd or Pb in forming a low-symmetry, nine-coordinate lattice structure[37], a result arising from its smaller ionic radius and the highly directional nature of its 3d orbitals (B. Kennedy, pers. commun.). Hence, the overall ability of Mn to be incorporated into the nacre of *H. depressa*, would not appear to be inconsistent with that demonstrated for Cd and Pb.

A major assumption implicit in the use of microlaminations as archival monitors of water chemistry, is that once an element is deposited in the shell, via the mantle, 1) it does not move out of the shell, or 2) migrate or diffuse into adjacent regions of the shell, thus smearing the signal originally recorded. We discount these possibilities for Mn in the present study because of the following reasons. Firstly, in a comprehensive study of the kinetics of several radionuclides, including ^{54}Mn, in the shell of the freshwater unionid bivalve *Velesunio angasi*, Harris[53] clearly showed that there was no significant ($p > 0.05$) loss of ^{54}Mn from the shell over 160 days, indicating a relatively long biological half-life (i.e. >320 days). Similarly, Mn has also been shown to have a relatively long biological half-life (i.e. >320 days) in the soft tissue of *V. angasi* (P. L. Brown, R. A. Jeffree and S. J. Markich, unpubl. results). This is due primarily to its low solubility as a hydrogen phosphate (HPO_4) salt in extracellular granules[54,55], even though these granules are bathed in the body fluids which would enhance the likelihood of leaching Mn from the tissue. Logarithms of the solubility products (log K_{sp}) of five divalent metal hydrogen phosphates show a positive, linear relationship ($p \leq 0.001$; $r^2 = 0.999$) with the log K_{sp}'s of the corresponding divalent metal carbonates (fig. 7), indicating a comparably low solubility of Mn in the shell.

Secondly, given the depositional structure of the shell nacre, where each incremental lamellae is isolated from the mantle fluids by a proceeding lamellae, it could be expected that the opportunity for the remobilisation of Mn, compared to the tissue, would be much less (except for lengthy anaerobic periods[30]). Indeed, since we predict that Mn will be bound predominantly at Ca^{2+} sites in the aragonite lattice of the shell nacre, as shown for Cd and Pb[46], it would have to migrate by a kind of diffusion process in the solid phase: a process generally not considered to be of any significance during the lifetime of the bivalve[56]. Therefore, Mn should not be particularly mobile relative to Ca, thus maintaining the integrity of the record of biomineralisation encoded by the Mn/Ca ratios.

Thirdly, is the interpretation that the depth profiles of normalised Mn signal intensities shown in figure 5a, 5b and 5c represent microlaminations rapidly reaching a steady state of passive entry/exit of Mn with the pallial fluid and homogenising with the shell interior, over 2 and 6 days of experimental exposure. However, if the process of diffusion was so rapid, then the period of several weeks that elapsed between the sacrifice of specimens at the end of the experiment and subsequent SIMS analysis, would lead to the disappearance of a profile of Mn in the nacre lamellae. This, however, was not apparent. Urey et al.[57] utilised $^{16}O/^{18}O$ ratios in fossil mollusc (belemnite) specimens to conclude that any diffusion would be negligible. Similarly, Tourtelot and Rye[58] found no evidence of post-depositional exchange, based on σ_c or $\sigma_c{}^{13}C$ (PDB) values, in the shell of fossil bivalves. Overall, using the above discussion as a rationale, we would expect a negligible movement of Mn either out of the shell or between adjacent microlaminations in the nacre.

Several studies have recognised that the ratios of Sr/Ca in the shells of a variety of aquatic molluscs are linearly related to the Sr/Ca ratios in the aquatic environment[29,42,59,60]. Moreover, this relationship has also been shown to hold for several other divalent metals, such as Mg, Ra, Cd, Pb, Cu and Zn[45,59-63], although only up to a certain metal/Ca ratio (see Simkiss[59]). Our results for Mn indicate that the ratio of Mn/Ca in the shell of *H. depressa* is reflecting the bioavailable concentration of Mn/Ca in the aquatic medium, a finding consistent with previous investigations of other divalent metals[29,59-63].

Acknowledgements. We thank Mr John Warmeant (ANSTO) for the preparation of shell material for SEM and SIMS, Mr Sammy Leung (ANSTO) for performing the SEM and Dr Jeff Huang (ANSTO) for XRD analysis of shell material. Mr Tim Tapsell (ANSTO) and Mrs Laura Edwards (ANSTO) are kindly thanked for their assistance in the preparation of many of the figures. We are also grateful to Dr Brendan Kennedy (Department of Chemistry, University of Sydney) for his helpful discussion during the study with respect to the shell mineralogy, and Mr Des Davy (ANSTO, retired) for his original suggestions on the study. We also acknowledge the Department of Industry, Science and Technology (DIST; Australian Government) for support of this work through the Bilateral Science and Technology Collaboration Program. The SIMS instrument in the University of Rouen was purchased with grants from the French 'Ministére de la Recherche et de la Technologie', 'the Region de Haute-Normandie' and CAMECA Company. Mr John Twining, Mr Ron Szymczak, Dr Peter Airey, Dr John Ferris, Dr Kathryn Prince (all from ANSTO) and Dr Graeme Batley (CSIRO Division of Coal and Energy Technology) are kindly thanked for providing constructive comments on an earlier manuscript.

1 Carell, B., Forberg, S., Grundelius, E., Henrikson, L., Johnels, A., Lindh, U., Mutvei, H., Olsson, M., Svärdström, K., and Westermark, T., Ambio *16* (1987) 2.
2 Lindh, U., Mutvei, H., Sunde, T., and Westermark, T., Nucl. Instrum. Meth. Phys. Res. *B30* (1988) 388.
3 Walker, K. F., Australian Water Resources Council Technical Paper No. 63. Australian Government Publishing Service, Canberra 1981.
4 Jeffree, R. A., Markich, S. J., and Brown, P. L., Aust. J. mar. Freshwat. Res. *44* (1993) 609.
5 Harrison, F. L ., and Quinn, D. J., Health Phys. *23* (1972) 509.
6 Auernheimer, C., Llavador, F., and Pina, J., Archs Sci., Genève *37* (1984) 317.
7 Brown, P. L. , Markich, S. J., and Jeffree, R. A., Radiochim. Acta. *66/67* (1994) 351.
8 Markich, S. J., and Jeffree, R. A., Aquat. Toxic. *29* (1994) 257.
9 Saunders, J., Scientific Services Report 91/31. Sydney Water Board, Sydney 1991.
10 Kerr, R., EPA Report 94/103. New South Wales Environment Protection Authority, Sydney 1994.
11 Brown, P. L., Haworth, A., Sharland, S. M., and Tweed, C. J., Nirex Safety Studies Report 188. U.K. Atomic Energy Authority, Harwell laboratory, Oxon 1991.
12 Verweij, W., Glazewski, R., and De Haan, H., Chem. Speciation Bioavailability *4* (1992) 43.
13 Rainbow, P. S., Malik, I., and O'Brien, P. O., Aquat. Toxic. *25* (1993) 15.
14 Thellier, M., Ripoll, C., Quintana, C., Sommer, F., Chevallier, P., and Danty, J., Meth. Enzym. *227* (1993) 535.
15 Stingeder, G., Anal. chim. Acta *297* (1994) 231.
16 Suzuki, S., Togo, Y., and Hikida, Y., J. geol. Soc. Japan *99* (1993) 1.
17 Anon., Powder Diffraction File. Inorganic phases, Sets 1–42. International Center for Diffraction Data, Swarthmore, Pennsylvania 1992.
18 Carter, J. G., in: Skeletal Growth of Aquatic Organisms: Biological Records of Environmental Change, pp. 69 and 627. Eds D. C. Rhoads and R. A. Lutz. Plenum Press, New York 1980.
19 Bourgoin, B. P., Mar. Ecol. Prog. Ser. *61* (1990) 253.
20 Watabe, N., in: The Mollusca, vol. 11, p. 69. Eds E. R. Trueman and M. R. Clarke. Academic Press, New York 1988.
21 Fritz, L. W., and Lutz, R. A., Veliger *28* (1986) 401.
22 Bourget, E., Bérard, H., and Brock, V., Can. J. Zool. *69* (1991) 535.
23 Caseiro, J., Dip. D. Thesis, l'Université Claude Bernard-Lyon I, France 1993.
24 Mook, W. G., and Vogel, J. C., Science *159* (1968) 874.
25 Lowenstam, H. A., and Weiner, S., On Biomineralisation. Oxford University Press, Oxford 1989.
26 Barrera, E., Tevesz, M. J. S., and Carter, J. G., Palaios *5* (1990) 149.
27 Dillaman, R. M., and Ford, S. E., Mar. Biol., Berlin *66* (1982) 133.
28 Jeffree, R. A., Verh. Int. Ver. Theor. Angew. Limnol. *23* (1988) 2193.
29 Rosenberg, G. D., in: Skeletal Growth of Aquatic Organisms: Biological Records of Environmental Change, p. 133. Eds D. C. Rhoads and R. A. Lutz. Plenum Press, New York 1980.
30 Crenshaw, M. A., in: Skeletal Growth of Aquatic Organisms: Biological Records of Environmental Change, p. 115. Eds D. C. Rhoads and R. A. Lutz. Plenum Press, New York 1980.
31 Simkiss, K., and Wilbur, K. M., (eds), Biomineralisation: Cell Biology and Mineral Deposition. Academic Press, New York 1989.
32 Fritz, L. W., Ferrence, G., and Jacobsen, T. R., Limnol. Oceanogr. *37* (1992) 442.
33 Carriker, M. R., Swann, C. P., Prezant, R. S., and Counts, C. L., Mar. Biol., Berlin *109* (1991) 287.
34 Simkiss, K., and Wilbur, K. M., in: Proceedings of the Tenth International Malacological Congress (Tübingen), Part 1, p. 1. Ed. C. Meier-Brook, Unitas Malacologica 1992.
35 Keith, J., Stockwell, S., Ball, D., Remillard, K., Kaplan, D., Thannhauser, T., and Sherwood, R., Comp. Biochem. Physiol. *105B* (1993) 487.
36 Blanchard, S. C., and Chasteen, N. D., J. phys. Chem. *80* (1976) 1362.
37 White, L. K., Szabo, A., Carkner, P., and Chasteen, N. D., J. phys. Chem. *81* (1977) 1420.
38 Naidu, Y. N., Rao, J. L., and Lakshman, S. V. J., Polyhedron *11* (1992) 663.
39 Pingatore, N. E., Lytle, F. W., Davies, B. M., Eastman, M. P., Eller, P. G., and Larson, E. M., Geochim. Cosmochim. Acta *56* (1992) 1531.
40 Stipp, S. L., Hochella, M. F., Parks, G. A., and Leckie, J. O., Geochim. Cosmochim. Acta *56* (1992) 1941.
41 Xu, N., Ph. D. Thesis, Stanford University, USA 1993.
42 Rosenberg, G. D., in: Skeletal Biomineralisation: Patterns, Processes and Evolutionary Trends, vol. 1. Ed. J. G. Carter. Van Nostrand Reinhold, New York 1990.
43 Berkman, P. A., Foreman, D. W., Mitchell, J. C., and Liptak, R. J., Antarct. Res. Ser. *57* (1992) 27.
44 Lorens, R. B., and Bender, M. L., Geochim. Cosmochim. Acta *44* (1980) 1265.
45 Blanchard, R. L., and Oakes, D. J., Geophys. Res. *70* (1965) 2911.
46 Lingard, S. M., Evans, D. A., and Bourgoin, B. P., Bull. Environ. Contam. Toxicol. *48* (1992) 179.
47 Wheeler, A. P., Rusenko, K. W., and Sikes, C. S., in: Chemical Aspects of Regulation of Mineralisation, p. 9. Eds C. S. Sikes and A. P. Wheeler. University of Alabama Publication Service, Mobile, Alabama 1988.
48 Greenfield, E. M., and Crenshaw, M. A., in: Origin, Evolution, and Modern Aspects of Biomineralisation in Plants and Animals, p. 303. Ed. R. E. Crick. Plenum Press, New York 1989.
49 Kawaguchi, T., and Watabe, N., J. Exp. Mar. Biol. Ecol. *170* (1993) 11.
50 Watabe, N., J. Ultrastruct. Res. *12* (1965) 351.
51 Smith, R. M., Martell, A. E., and Motekaitis, R. J., NIST Critical Stability Constants of Metal Complexes Database, Version 1, National Institute of Standards and Technology, Gaithersburg, Maryland 1993.
52 Onuma, N., Masuda, F., Hirano, M., and Wada, K., Geochem. J. *13* (1979) 187.
53 Harris, J., M. App. Sc. Thesis, University of Technology, Sydney, Australia 1990.
54 Jeffree, R. A., and Simpson, R. D., Comp. Biochem. Physiol. *79A* (1984) 61.
55 Jeffree, R. A., in: Proceedings of a Bioaccumulation Workshop: Assessment of the Distribution, Impacts and Bioaccumulation of Contaminants in Aquatic Environments, p. 225. Ed. A. G. Miskiewicz. Sydney Water Board and Australian Marine Sciences Association Inc, Sydney 1992.
56 Sturesson, U., Ambio *7* (1978) 122.

57 Urey, H. C., Lowenstam, H. A., Epstein, S., and McKinney, C. R., Bull. geol. Soc. Am. *62* (1951) 399.
58 Tourtelot, H. A., and Rye, R. O., Bull. geol. Soc. Am. *80* (1969) 1903.
59 Simkiss, K., in: Biomineralisation and Biological Metal Accumulation, p. 363. Eds P. Westbrook and E. W. de Jong. D. Reidel Publishing Co., Dordrecht 1983.
60 Rio, M., Roux, M., Renard, M., and Schein, E., Palaios *7* (1992) 351.
61 Fang, L-S., and Shen, P., Mar. Ecol. Prog. Ser. *18* (1984) 187.
62 Sturesson, U., in: Ecotoxicological Testing for the Marine Environment, vol. 2, p. 511. Eds G. Persoone, E. Jasper and C. Claus. State University of Ghent and Institute of Marine Scientific Research, Bredene, Belgium 1984.
63 Krantz, D. E., Kronick, A. T., and Williams, D. F., Paleogeogr. Paleoclimatol. Paleoecol. *64* (1988) 123.